Artificial Iono- and Photosensitive Membranes Based on an Amphiphilic Aza-Crown-Substituted Hemicyanine

Pinar Batat, Christine Grauby-Heywang, Sophiya Selektor, Daria Silantyeva, Vladimir Arslanov, Nathan Mcclenaghan, Gediminas Jonusauskas

Artificial Iono- and Photosensitive Membranes Based on an Amphiphilic Aza-Crown-Substituted Hemicyanine

Pinar Batat,*[a, b] Christine Grauby-Heywang,[a] Sophiya Selektor,[c] Daria Silantyeva,[c] Vladimir Arslanov,[c] Nathan McClenaghan,[b] and Gediminas Jonusauskas[a]

Artificial iono- and photosensitive membranes based on an amphiphilic aza-crown-substituted hemicyanine are assembled on liquid and solid supports and their aggregation behaviour, which is influenced by the binding of metal cations and surface density, is studied. The photoinduced charge-transfer properties of an analogous non-amphiphilic hemicyanine in solution are also dmonstrated. An asymmetric sandwich dimer model is proposed and existence of such dimers in solution is evidenced by transient absorption and fluorescence anisotropy experiments. Changes in absorption and emission spectra, as well as compression isotherms of the amphiphile observed in the presence of cations, are discussed in terms of 2D molecular reorganisation. Surface-pressure-controlled reversible excimer formation at the air–water interphase and excimer-type emission of Langmuir–Blodgett films in the presence of cations are demonstrated and are discussed on the basis of fibre-optic fluorimetry and fluorescence microscopy results.

1. Introduction

Hemicyanines are organic dyes that are used in many applications, including fluorescent sensors,[1–3] labels[4–7] and probes,[8,9] and laser dyes.[10–12] They are known to readily self-aggregate, which can present a problem in some applications. This aggregation depends on the structure of the dye and on environmental factors such as pH, temperature, solvent polarity, concentration and ionic strength of the hemicyanine solution.[13]

For some applications, it is necessary to organise hemicyanines in 2D films, such as Langmuir–Blodgett (LB) films. In order to achieve this, amphiphilic hemicyanines bearing a hydrophobic chain are required. These films could be used to design light-sensitive functionalised artificial membranes. Hemicyanines used in this way have become powerful molecular tools for optical reading of electrical activity in neurons, revealing fast change in their cell-membrane voltage, as shown in membrane models.[14]

Other applications might also require ionophores to be conjugated to hemicyanines, for example, crown ethers that are able to selectively bind cations. The specificity of the cation–crown interaction is related to the nature of heteroatoms that form the crown and the size of the cavity. The binding of a cation by a crown ether that is connected to the π-conjugated system of a dye typically changes the optical properties (absorption and fluorescence emission) of the conjugate; these changes being useful for the detection of the cation. One of the most important cations in living organisms is Ca^{2+}, which is an essential second messenger. Changes in its intra- and extracellular concentrations are responsible for many biological processes.[15] For this reason, large numbers of studies have been devoted to the sensing of Ca^{2+}, especially in aqueous media.[16] In addition to cation sensing, another important aspect of interactions between cations and chromoionophores is the possibility of combining two molecules (monomers) to form dimers (excimers). These aspects of aggregation behaviour are important in the design of molecular switches for both 3D systems (solutions) and organised films on liquid and solid substrates.

In the present work, the properties of a crown-substituted hemicyanine dye were investigated in solvents with different dielectric constants, and in Ca^{2+}- and Ba^{2+}-containing solutions. Various complementary methods were used, such as electronic absorption spectroscopy, steady-state and time-resolved fluorescence spectroscopies, surface-pressure measurements and fluorescence microscopy. Understanding the ion-sensitive properties of hemicyanine films is also the starting point for the development of cation-specific sensors in the condensed phase.

This study addressed the formation of monolayers and LB films of an amphiphilic analogue of an aza-crown-substituted hemicyanine, and the microstructure of these ultrathin films in the absence or the presence of two different cations: Ca^{2+}, which is able to enter the crown ether cavity, and Ba^{2+}, which is too large to bind inside the crown.

[a] *Dr. P. Batat, Dr. C. Grauby Heywang, Dr. G. Jonusauskas*
LOMA Université de Bordeaux, UMR CNRS 5798
351, crs de la Libération 33405 Talence (France)
Fax: (+33) 05 4000 6970
E mail: pinarbatat@hotmail.com

[b] *Dr. P. Batat, Dr. N. McClenaghan*
ISM Université de Bordeaux, UMR CNRS 5255
351, crs de la Libération 33405 Talence (France)

[c] *Dr. S. Selektor, D. Silantyeva, Prof. V. Arslanov*
Frumkin Institute of Physical Chemistry and Electrochemistry RAS
31 4, Leninsky prospect, ZIP 119071,
Moscow (Russian Federation)

2. Results and Discussion

2.1. Studies in Solution

Knowledge of the molecular electro-optical parameters, such as dipole moments or polarisability, is useful in designing nonlinear optical materials. These parameters can be determined by using semi-empirical molecular orbital calculations or by analysing the spectral shifts observed in the presence of solvents with different macroscopic parameters, such as electric permittivity and refractive index. Thus, spectral characteristics of an ionophore–hemicyanine conjugate (**C1**, Figure 1) and its photoinduced charge-transfer (PCT) properties were studied in solvents with different dielectric constants (see Figure S1 in the Supporting Information for fluorescence spectra). A summary of steady-state measurements is presented in Table 1. As often observed for these types of dyes, the emission is red shifted with increasing solvent polarity (positive solvatochromism).[17] However, the complex behaviour of **C1** in water does not fit this trend—the low extinction coefficient suggests that dye molecules aggregate, and the contribution of hydrogen bonding also complicates an otherwise simple interpretation of the data.

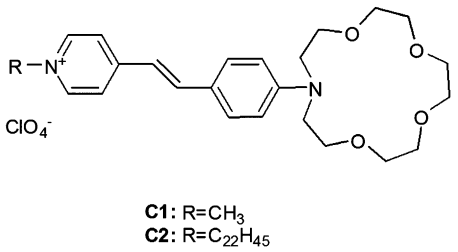

C1: R=CH_3
C2: R=$C_{22}H_{45}$

Figure 1. Structures of the ionophore hemicyanine conjugates in this study: **C1** and **C2**.

According to the Lippert–Mataga theory,[18,19] the ground-state and excited-state dipole moments of a molecule are dependent on solvent polarity.[20] Upon excitation of the chromophore, a net displacement of electron density occurs from the electron-lone-pair-bearing amine group towards the electron-poor pyridinium moiety. This displacement results in changes of the ground- and excited-state dipole moments. According to the Lippert equation, it is possible to calculate the difference of ground- and excited-state dipole moments from the slope of the graph of the difference between the absorption and emission maxima (ν_A–ν_F) versus the Lippert–Mataga parameter (Δf_{LM}). Figure 2 shows the results obtained in the case of **C1**. The ground- and excited-state dipole moments were calculated, by using molecular orbital package (MOPAC) software,[21] to be 17.7 and 2.3 D, respectively, whereas the difference from fitting experimental data was found to be approximately 11 D. This result was expected, because the molecule is a cationic dye and already polar in the ground state. The difference between theoretical and experimental values is more likely due to the use of a Franck–Condon excited state for calculations and to neglecting specific solvent–solute interactions in the both ground and excited states. This information would prove useful in designing new materials, in our case artificial membranes, with nonlinear optical properties.

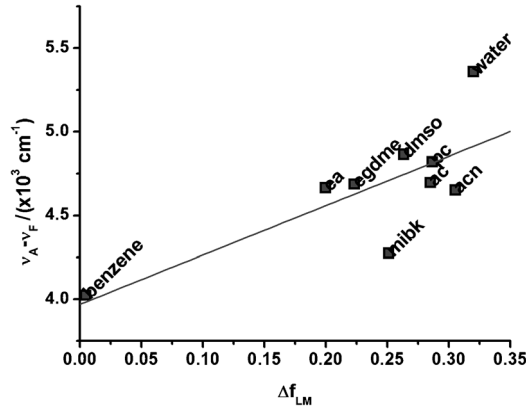

Figure 2. Difference between the absorption and emission maxima (ν_A ν_F) of **C1** versus the Lippert Mataga parameter (Δf_{LM}).

Table 1. Spectral characteristics of **C1** in solvents of increasing polarity, as determined by their relative dielectric constant (D), wavelength of maximum absorption (λ_{abs}) and fluorescence emission (λ_{fluo}), Stokes shift, molar extinction coefficient (ε) and fluorescence quantum yield (Φ_{fluo}).

Solvent[a]	λ_{abs} [nm]	λ_{fluo} [nm]	D	Stokes shift [cm ^{1}]	ε [M ^{1}L ^{1}]	Φ_{fluo} (×10^2)
benzene	474	601	2.3	4022	24100	7.6
EA	470	602	6.02	4665	23000	8.2
EGDME	478	616	7.2	4686	45100	4.8
MIBK	487	615	13.11	4273	46300	3.6
AC	479	618	20.56	4695	50300	1.3
ACN	474	617	35.92	4783	42500	1.4
DMSO	474	616	46.45	4863	42000	7.2
PC	475	616	64.92	4818	40400	4.3
water	454	600	80	5359	20300	1.2

[a] Abbreviations: EA, ethyl acetate; EGDME, ethylene glycol dimethyl ether; MIBK, methyl isobutyl ketone; AC, acetone; ACN, acetonitrile; DMSO, dimethyl sulfoxide; PC, propylene carbonate.

Notably, the conjugated electron system of **C1** was sensitive not only to solvent polarity but also to metal cations, which can be bound by the crown ether moiety. The complexation of Ca^{2+} and Ba^{2+} by **C1** was studied in acetonitrile. As shown in Figure 3, the electronic absorption spectrum was strongly modified upon **C1** interacting with both cations. The main lowest-energy absorption band was blue shifted from 474 to 370–390 nm in the presence of cations and its intensity decreased; this reflects the reduced influence of the amine electron density on the PCT system when it is involved in cation binding.

The following equilibria were considered in fitting the absorption spectra using the SPECFIT/32 program[22] (L = **C1**, M = Ca^{2+}, Ba^{2+}):

For both cations, the determined binding constant for 2:1 complexation (K_{21}) in acetonitrile was around 10^7 M^{-1}, whereas

$$2L + M \overset{K_{21}}{\longleftrightarrow} L_2M \qquad K_{21} = \frac{[L_2M]}{[L]^2\,[M]}$$

$$L + M \overset{K_{11}}{\longleftrightarrow} LM \qquad K_{11} = \frac{[LM]}{[L]\,[M]}$$

the 1:1 complexation (K_{11}) was too low for reliable fitting of data.

Taking into account the fact that the aza-crown moiety has one binding site, a 1:1 complex with Ca^{2+} was expected. Such complexation should cause the absorption bands corresponding to the free ligand (hemicyanine) to disappear and a single blue-shifted spectral band for the complex to rise. In contrast to this expectation, the spectrum of the complex was found to have a complicated bimodal structure. This observation led to the conclusion that another type of complex had appeared in solution,[23] the simplest hypothesis being a "sandwich" dimer model, in which two hemicyanine molecules share one cation. As two bands are observed, this suggests that one of the molecules is less affected than the other, probably because the cation is positioned asymmetrically with respect to the two ligands. Under these conditions, the least affected amine group gives rise to the absorption band at 470 nm and the other, more affected, **C1** ligand has a corresponding blue-shifted band. Moreover, the emission band observed after an excitation of either of these two bands is around 610 nm (data not shown), corresponding to the Stokes shift from the blue absorption-band position of approximately 10500 cm^{-1}. This dramatic shift comes from lowering the HOMO–LUMO energy gap of the complex to that of the free ligand. This drop can be explained in two ways: the decomplexation of the cation or energy transfer from the ligand with the higher excited-state energy level to the ligand with the lower one, this transfer being followed by the fluorescence emission.

To better understand the behaviour of these complexes, pump–probe experiments on the ps timescale were performed. Figure 4 shows the 2D transient absorption map and selected spectra of the Ca^{2+} complex at different time delays. A positive band with a maximum at 450 nm and a negative band between 500–650 nm, which have the same decay time of 270 ps, were observed. No other transient features were found. The positive band is assigned to the excited-singlet-state absorption and the negative band is the stimulated emission band. A decomplexation process in similar systems was readily observed in ultrafast pump–probe spectroscopic experiments, and is characterised by important displacements of transient absorption bands in the time delay range of a few ps.[24,25] As no spectral changes were observed on this timescale, the energy transfer between dimer molecules appears to be a more probable phenomenon. Homo transfer was faster than hetero transfer, due to more available orientation and intermolecular distances as a result of structural similarities.[26]

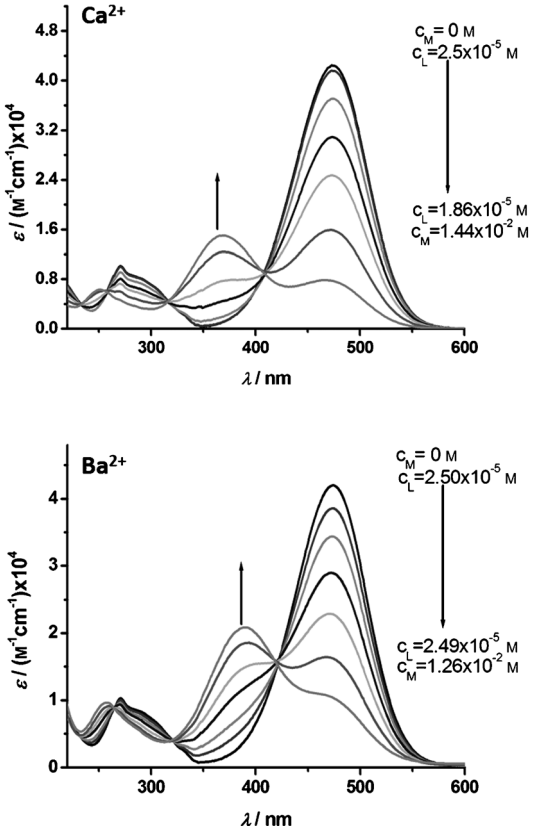

Figure 3. Changes of absorption spectra of **C1** upon titration with Ca^{2+} (top) and Ba^{2+} (bottom). Spectra recorded in acetonitrile (L = hemicyanine ligand, M = cation).

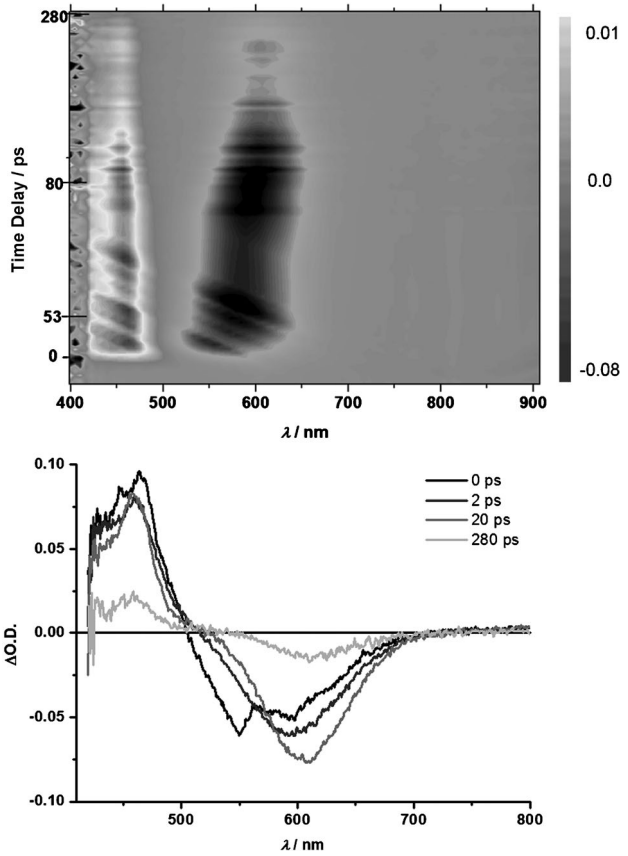

Figure 4. Transient absorption of **C1** Ca^{2+} complex ([**C1**] = 2.10 ^{5} M, [Ca^{2+}] = 1.5.10 ^{2} M) in acetonitrile (λ_{exc} = 360 nm). O.D.: optical density.

This might mean that the energy transfer in this system occurs at a shorter time scale than our experimental resolution.

The stimulated emission was shifted bathochromically with increasing time delay (Figure 4). Figure 5 presents the variation in the position of the stimulated emission maximum that depends on the pump–probe time delay. In addition, fluorescence lifetime measurements are presented in Figure S2 and Table S1. The lifetime of the stimulated emission shift was determined to be 120 ps. This time constant is too long to be assigned to the solvation of molecules, which in acetonitrile, occurs within 200 fs.[27]

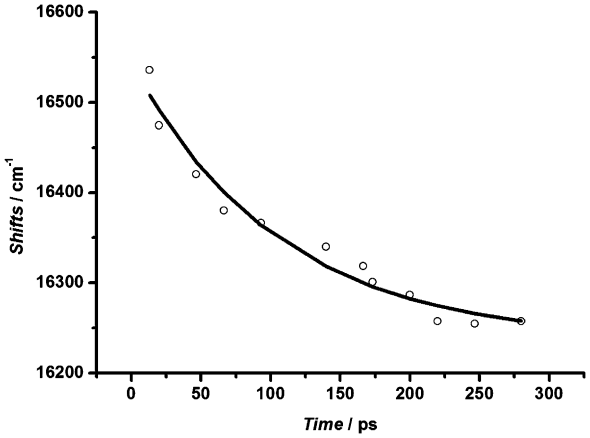

Figure 5. The Stokes shifts of the stimulated emission band of **C1** Ca^{2+} versus time delays.

Fluorescence anisotropy experiments were performed to validate the sandwich dimer model. The results were treated using the Langevin equation (see the Experimental Section), which describes the relationship between the fluorescence anisotropy decay time and the moment of inertia of the emitting dipole. The moments of inertia can be calculated by using CHEM3D software. Figure 6 shows that this relationship is linear for various molecules in acetonitrile, and the slope is related to the microscopic friction of acetonitrile. The hypothesis of rotation of a dimer formed by slightly shifted and parallel **C1** molecules (Figure 6, inset) was not in good agreement with the slope of the graph. However, the dimer model, in which one of the molecules rotates about the plane of the aza-crown (Figure 6, inset), fits well. The flexibility of the ligand allows separation of the two positive charges of the complex, thus decreasing electrostatic repulsion. Electrostatic interaction with perchlorate counter anions to give an overall neutral complex, is also not excluded. Furthermore, the fact that Ba^{2+} and Ca^{2+} cations behave similarly appears contradictory to previous reports on aza-crown-containing dyes. For example, Mateeva et al. proposed the formation of 1:1 complexes between Ca^{2+} and a 15-aza-crown-containing dye in solution, and that these complexes are more stable than those containing Ba^{2+}.[23] However, the dye conjugated to the crown in that study has different electronic distributions from the dye studied here, which might strongly affect the properties of the complex.

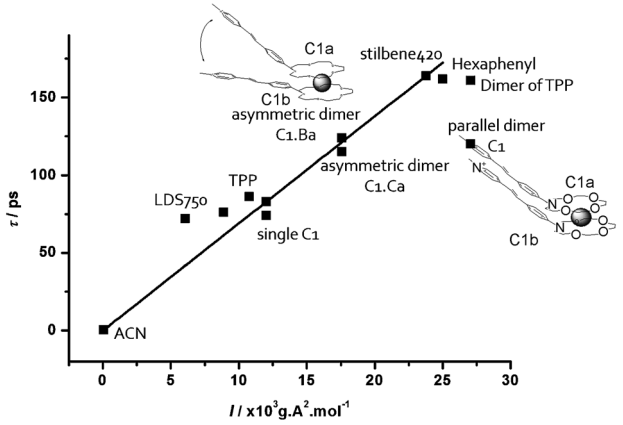

Figure 6. The anisotropy decay time versus the moment of inertia for different compounds in acetonitrile. Stilbene 420: 2,2′ ([1,1′ biphenyl] 4,4′ diyldi 2,1 ethenediyl)bis benzenesulfonic acid, disodium salt; LDS750: 2 [4 [4 (dimethylamino)phenyl] 1,3 butadienyl] 3 ethyl naphtho[2,1 *d*]thiazolium perchlorate; TPP: 5,10,15,20 tetraphenylporphyrin.

Finally, these results can be explained by considering the energy transfer between molecules in the dimer. The molecule possessing the higher HOMO–LUMO energy gap in the dimer is excited by the absorption of the photon. Over a short time period (a few tens of fs), energy transfer occurs towards the molecule possessing the lower gap. This excited molecule subsequently relaxes by fluorescence emission. This relaxation is accompanied by the separation of the sandwich by the rotation of the excited molecule about its aza-crown, which causes the anisotropy decay of fluorescence emission within 120 ps for both cations. The shift of the stimulated emission band in the transient absorption signal also has the same time constant. In this situation, the influence of the non-excited molecule on its excited neighbour is reduced continuously, and the solvent around the molecule has an increasing effect on the excited energy levels by penetrating the free space between the increasingly separated molecules.

2.2. Studies of Self-Assembly

To assess the prospects of using a hemicyanine dye as a basis for ultrathin membranes, we investigated the conditions required to produce stable, ordered LB films of **C2**, and the influence of Ba^{2+} and Ca^{2+} on the optical properties and structure of such films. The high reproducibility of compression isotherms and a weak dependence of their position and initial molecular area (which changed twofold) on solution concentrations (which varied from 2×10^{-4}–1×10^{-3} M) indicate that **C2** forms stable monolayers at the air–water interface.

The π–A isotherm of the monolayer spread over pure water (Figure 7, 0 mM) showed first a regular and monotonous increase of the surface pressure with compression at molecular areas from 130 to 75 Å^2. At a molecular area of 75 Å^2, an inflection of the isotherm, followed by a well-defined plateau, was observed: the surface pressure remained almost constant around 15 mN m^{-1} down to a molecular area of 40 Å^2. Further compression induced a steeper increase of surface pressure as

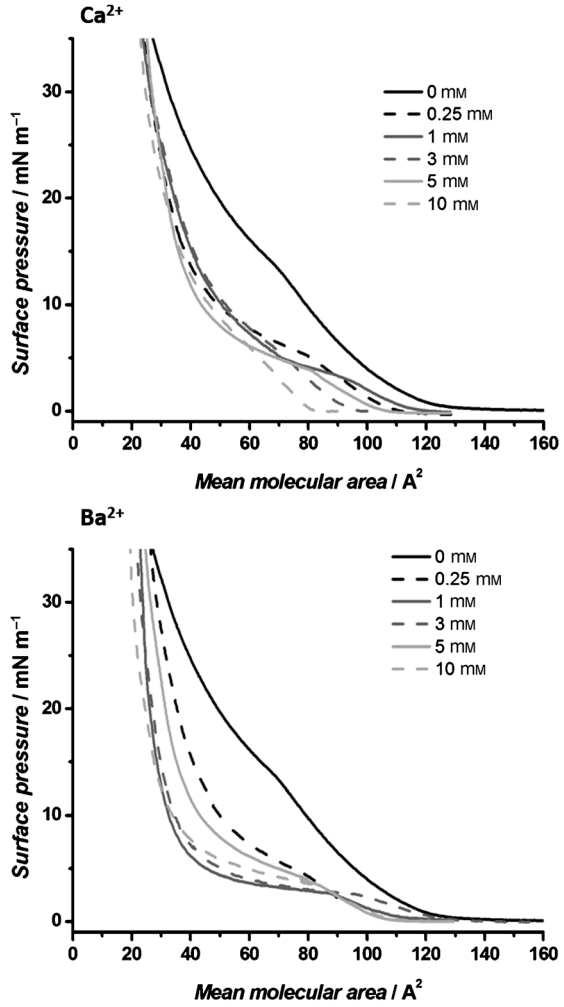

Figure 7. Isotherms of monolayers of **C2** on a pure water subphase or on aqueous solution containing Ca^{2+} (top) and Ba^{2+} (bottom).

compared to the initial isotherm, and the final mean molecular area is around 20 Å^2. If we consider that in the ideal case, the estimated areas of horizontally (face-on) and vertically (edge-on) oriented molecules are 130 and 20 Å^2 (with the crown fragments immersed in the water), respectively, this behaviour can be attributed to the reorientation of **C2** molecules upon compression. Notably, the horizontal face-on orientation of the molecules at the air–water interface at the start of compression ($\approx$130 Å^2) gradually became vertical (edge-on) in the plateau area. At a surface pressure higher than 20 mN m^{-1}, a close-packed edge-on arrangement was reached.

The presence of Ca^{2+} or Ba^{2+} in the subphase (0.05–10 mM) induced changes in the isotherm, as shown in Figure 7 top and bottom, respectively. By increasing the concentration of Ca^{2+} into the subphase, the onset of π growth was shifted towards a lower area per molecule. For example, growth started at 110 Å^2 at 0.05 mM, 90 Å^2 at 3 mM and 82 Å^2 at 10 mM of Ca^{2+}. By increasing the Ba^{2+} concentration in the subphase, we observed an effect similar to that with Ca^{2+}—the onset value was also shifted to lower area per molecule, albeit in a less pronounced way: for example, 130 Å^2 for 3 mM and 105 Å^2 for 5 mM.

Another change was related to the general shapes and slopes of the isotherms. Overall, an increase of salt concentration decreased the surface-pressure range of the plateau. If we suppose that the first part of the isotherm at high molecular areas is related to the monolayer in a somewhat loose molecular organisation, then the implication is that the presence of salt brings molecules closer and rigidifies the monolayer. However, the orientation of molecules at the end of the compression appeared to be similar in the absence and presence of cations, even though a wider range of molecular areas was observed in the case of Ca^{2+}, as compared to Ba^{2+}, at the end of the compression.

The observed changes of the **C2** compression isotherms in the presence of cations complementary to the aza-crown ether were similar to those previously found for a dithia-aza-crown-conjugated hemicyanine dye in the presence of Hg^{2+} in the subphase.[28] In that study, the formation of a complex between Hg^{2+} and a dithia-aza-crown-ether group was demonstrated unambiguously.[28] This indicates that in **C2**, the monolayer structure might also vary as a result of an interaction of the cations with the ionophore.

All these results suggest that the organisation of hemicyanine molecules at the air–water interface changes in the presence of Ca^{2+} and Ba^{2+}. However, the analysis of isotherms alone is not sufficient to describe these changes at the molecular level; other, especially spectroscopic, data (vide infra) are required.

The absorption spectra of the **C2** monolayer measured during its compression with different subphases are shown in Figure 8. In the case of the monolayer on a pure water subphase before compression (0 mN m^{-1}), two bands are observed in the absorption spectrum. These bands, at 480 and 272 nm, correspond to the $S_1 \leftarrow S_0$ and $S_2 \leftarrow S_0$ transitions, respectively. Upon monolayer compression, the first band shifts to 450 nm. The blue shift of the $S_1 \leftarrow S_0$ transition upon compression suggests the formation of H aggregates of the hemicyanine in the monolayer[29] (such aggregation can also be observed in some solvents, owing to the low solubility of hemicyanines). In the presence of both Ca^{2+} and Ba^{2+} (even at a low concentration), the main band was, on the contrary, red-shifted to 500 nm under compression (Figure 8, bottom).

The absorption spectra of monolayers transferred onto silica plates at a constant surface pressure of 30 mN m^{-1} are shown in Figure 9. A sufficiently high surface pressure is necessary to maintain molecular cohesion during transfer from the air–water interface to the substrate. Overall, these spectra are similar to those of corresponding monolayers at the end of compression and their intensity decreases slightly with increasing cation concentration. Simultaneously, a new band centred in the 370–390 nm region appears as a small shoulder on the edge of the band at 500 nm. The position of this new band is similar to that of the band previously observed in the case of complexation in solution (see Figure 3).

The Ba^{2+} cation is larger than Ca^{2+}, and as a consequence, unlike Ca^{2+}, it does not fit into the crown cavity of **C1**.[23] Therefore, the hemicyanine monolayers were anticipated to be affected differently by the presence of these two cations. How-

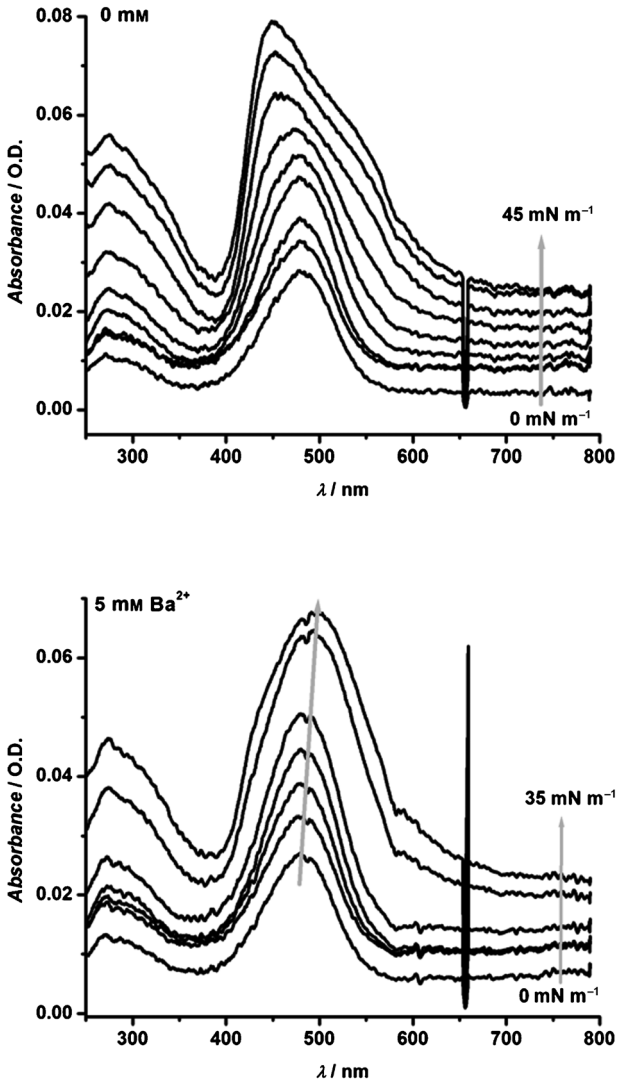

Figure 8. Absorption spectra of **C2** monolayer during its compression on a pure water subphase (top) or on an aqueous solution containing 5 mM Ba^{2+} (bottom).

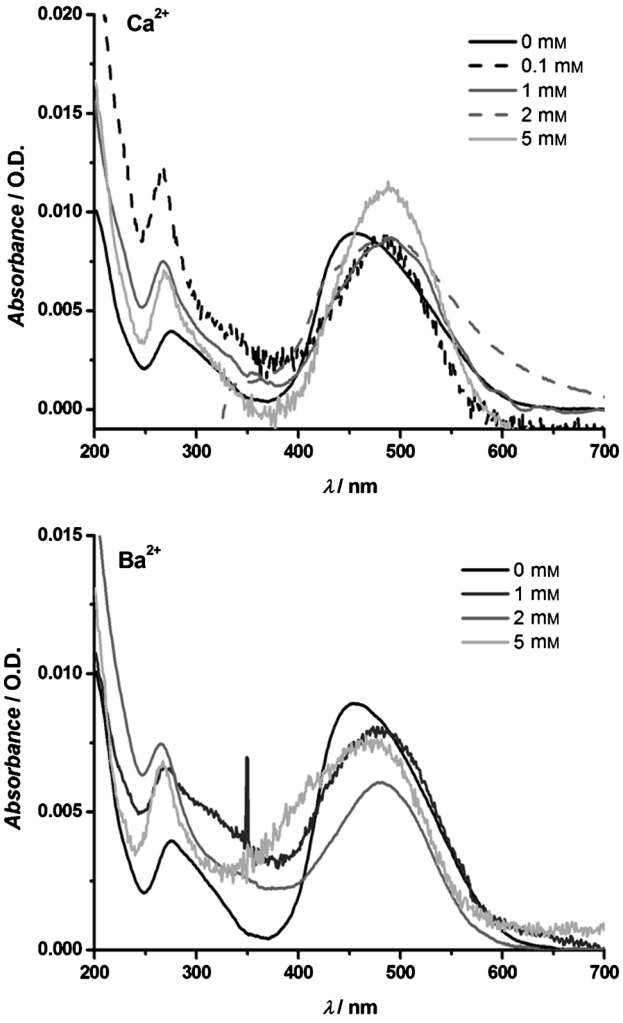

Figure 9. Absorption spectra of single layer LB films of **C2** on silica transferred at 30 mN m ^{1} from pure water subphase or aqueous solution containing Ca^{2+} (top) and Ba^{2+} (bottom).

ever, notable disparities were not observed in either the isotherms or the absorption spectra.

The red shift of the main absorption band is clearly due to the presence of cations, thus suggesting that an interaction of these cations with **C1** occurs even at the lowest cation concentrations, as previously suggested by surface-pressure measurements. This interaction also prevents the formation of H aggregates. The band appearing as a small shoulder at 370–390 nm is another indication of the cation–hemicyanine interaction.

However, owing to low values of binding constants for these complexes in aqueous solutions,[23] it would be incorrect to assume formation of a stable complex. In our previous study,[28] no spectral indications of complex formation in **C2** (Figure 1) monolayers were found at the air–water interface and in LB films at high concentrations of Ba^{2+} in the subphase (5–10 mM).

To reveal the role of surface pressure in the evolution of emission spectra upon monolayer compression, fluorescence was measured in situ directly at the air–aqueous subphase interface. Figure 10 shows, for example, changes induced by surface pressure in the fluorescence spectra of hemicyanine monolayers spread on a subphase containing 1 mM Ca^{2+}. At low surface pressure, the emission of monomers was observed at around 620 nm. Upon increasing the surface pressure, the monomer emission decreased and a new red-shifted band at 700 nm appeared, possibly owing to molecule pairs (excimer emission). Moreover, the first signs of the excimer emission appeared at a surface pressure that corresponds to the beginning of the plateau on the isotherm upon straightening of the molecules. Notably, no excimer formation was detected on a pure water subphase. In the cation-containing subphase, there is competition between water molecules and cations for the crown, and in the presence of chloroform the cations dominate. Evidently, the presence of chloroform at the initial stage of monolayer formation favours the extraction of cations from water to the crowns,[30] which allows formation of the initial sandwiches responsible for the monolayer structure and excimer-type fluorescence. After evaporation of chloroform, the

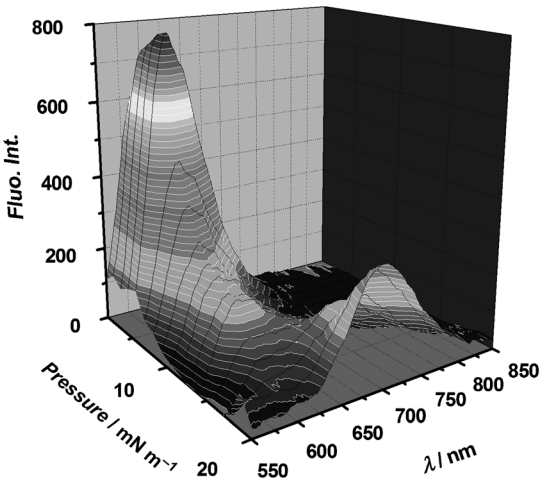

Figure 10. Emission spectra of **C2** monolayers at the air water interface at different surface pressures. The subphase contained 1 mM Ca^{2+}.

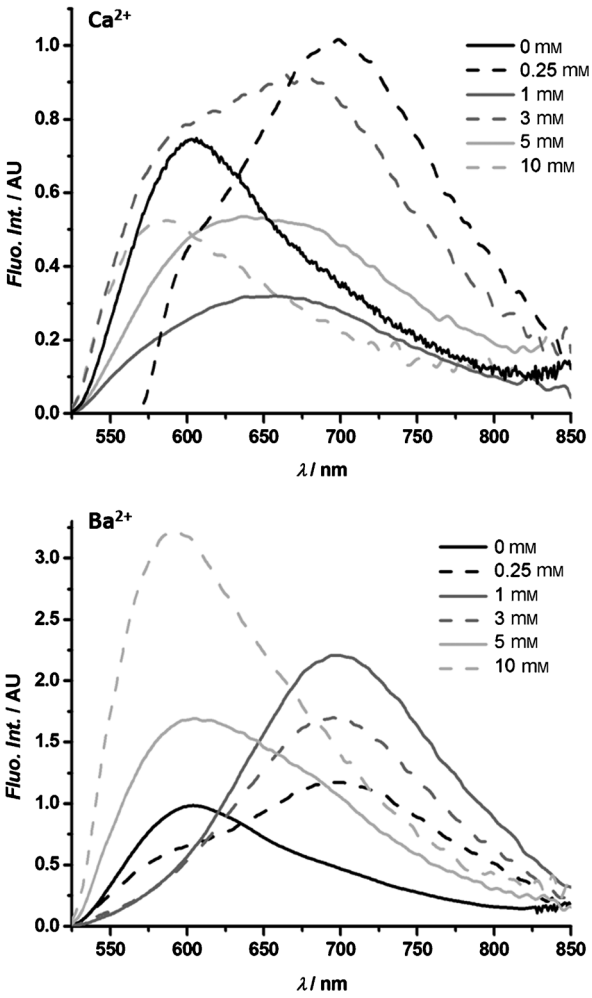

Figure 11. Fluorescence spectra of single layer LB films of **C2** on silica trans ferred at 30 mN m ^{1} from pure water and subphases with different Ca^{2+} (top) and Ba^{2+} (bottom) concentrations.

hydration of the crown ether ejects cations from the monolayer.[31] That might explain why there are not any significant spectral indications of complex formation in **C2** monolayers. However, sandwich-type dimers formed at this stage are retained after the evaporation of chloroform. As expected, the fluorescence spectra of monolayers at 30 mN m^{-1} are similar to those of the corresponding LB films.

Figure 11 shows the fluorescence spectra of LB films transferred from pure water or subphases containing different concentrations of Ca^{2+} and Ba^{2+} (Figure 11, top and bottom, respectively). In the case of pure water, an emission band is observed at 600 nm. In the presence of both cations, at concentrations lower or equal to 5 mM, two emission bands are observed at 600 and 700 nm, with different intensity ratios. At high cation concentration (10 mM), a single band at 575 nm is observed.

As mentioned above, cations inhibit the H-aggregation process in the monolayer (Figure 8), although they are probably involved in sandwich dimer formation in solution. We tentatively propose a similar organisation in monolayers and LB films—at least for cation concentrations below 5 mM—which seems to be preferred for 2:1 complexation. The compression of the monolayer induces orientation and provides closely packed pre-formed dimers at the air–water interface. It is evident that such organisation favours the formation of excimers, characterised by a greatly red-shifted fluorescence emission around 700 nm. The other band observed at different cation concentrations might be due to the presence of monomers not involved in excimer formation. Furthermore, at 10 mM cation, the unique blue-shifted emission band at 575 nm might be due to a new molecular organisation induced by the high cation concentration.

Surface pressure and spectroscopic measurements provide information on the organisation of molecules within LB films (monomer, aggregate, excimer). However, it is useful to complement this information by directly observing their morphology. Hemicyanines are intrinsically fluorescent, therefore fluorescence microscopy is particularly suitable, as no additional label is needed.

The fluorescence images (Figure 12) support our previous hypotheses about the effect of cations on monolayer and LB film structures. Image 1, corresponding to LB films transferred from pure water, is uniform at the resolution of the fluorescence microscope, in agreement with homogenous H aggregation of molecules into the films, although some defects do appear, probably owing to imperfections in the surface of the substrates. In the presence of cations, heterogeneities appear in the LB films (Figure 12, Image 2). Finally, Image 3, corresponding to a transfer from water containing 10 mM Ba^{2+}, again shows a homogenous surface, in accordance with the molecular organisation induced by the high cation concentration, mentioned previously in the fluorescence emission study of these samples.

Overall, the organisation of hemicyanine molecules in LB films can be summarised as follows: at the air–water interface, owing to surface-pressure-induced organisation, hemicyanine conjugates are able to straighten and form H aggregates. Indeed, the solvation of molecules in pure water provides fa-

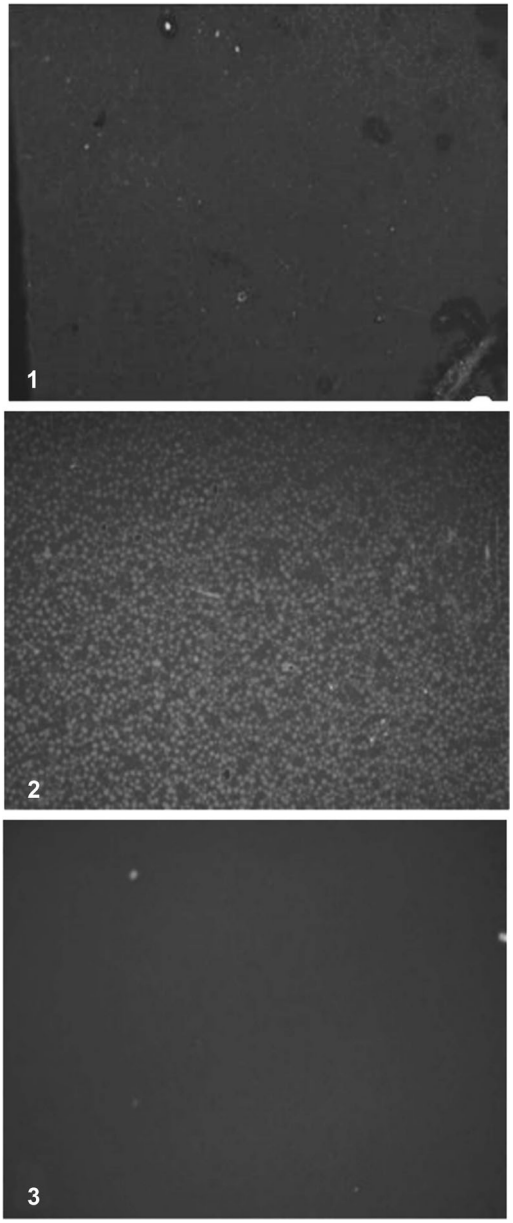

Figure 12. Fluorescence microscopy images of single layer LB films transferred at 30 mN m^{-1} (for all images: excitation at 470–490 nm, emission above 520 nm, dimensions: 700 μm × 520 μm). Image 1: LB film transferred from pure water. Images 2 and 3: LB films transferred from water containing Ba^{2+} cations at 0.5 mM and 10 mM, respectively.

vourable conditions for H-aggregate formation. On the other hand, upon introduction of even a low concentration of cations, this type of aggregation is inhibited. However, the presence of chloroform must be also taken into account. As described previously, upon spreading the dye solution at the interface between air and the aqueous cation solution, chloroform induces the extraction of cations from water to the crown ethers. Further hydration of crown ether groups after evaporation of chloroform ejects cations from the monolayer, although sandwich-type dimers formed initially are retained.

Hemicyanine monolayers behave similarly in the presence of Ca^{2+} and Ba^{2+}, whereas the latter has a greater volume and is not expected to fit into the crown. We did not observe noticeable disparities, either in isotherms or in absorption and emission spectra. The only difference between the two cations concerns the concentration range necessary to induce a specific effect. If we consider that there is no formal complexation (one cation fitting exactly into the crown) at cation concentrations ≤ 5 mM, our results can be explained by the formation of sandwich dimers (Figure 13) in the presence of chloroform at the

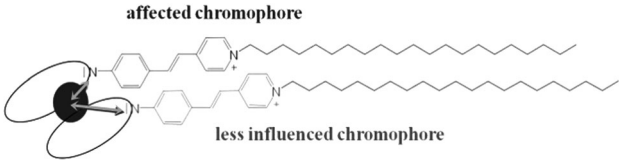

Figure 13. Formation of a sandwich dimer with Ba^{2+} or Ca^{2+} at low concentration.

beginning of spreading (as discussed previously, chloroform would cause the crown–cation interaction to be favoured). On the contrary, we can suppose that chloroform evaporation induces the opposite effect, as it would be accompanied by hydration of crown-ether groups, followed by the disassembly of the complexes. However, even if cations are released back into the subphase, we can assume that the initial sandwiches act as nuclei for the formation of domains, leading to the resulting structures observed using fluorescence microscopy. The sandwich geometry would also be responsible for the decrease of molecular areas observed on π–A isotherms at low surface pressure compared to those obtained on a subphase of pure water. Moreover, under compression, this new type of monolayer organisation would lead to the formation of structures with an excimer-type emission (Figure 10). Such structures were maintained on silica plates (Figure 11). The two cations differed only in the concentration range necessary to induce this specific effect (approximately 0.1 mM Ca^{2+} and 1 mM Ba^{2+}). A strong cation–crown interaction in the presence of chloroform (thus a high binding constant) implies that a low concentration of cations is required to form the initial sandwiches responsible for the excimer-type fluorescence. This explains the difference in concentration of the two cations necessary to induce this specific effect.

Based on the results described above, a supramolecular structure responsible for the excimer-type emission can be proposed. Such structures could be a result of parallel packing of dye molecules similar to that of H aggregates. The presence of cations in the subphase would favour the sandwich-type structures, in which one molecule in the sandwich is offset slightly from the other, owing to the angle between the planes of the crown and the chromophore at the amine group (Figure 13). Such a structure did not show any excimer-based emission in solution. However, in monolayers, another intermolecular interaction, favourable for excimer formation, might be acting between two adjacent molecules belonging to two neighbouring sandwiches.

Furthermore, although sandwich dimers are observed for both cations, their behaviour differs with respect to the cation, apparently because of the difference in binding constants.[23] Indeed, if the crown–cation interaction is stronger, a low concentration of cation is necessary to induce excimer formation. Our results confirm the importance of the binding constant, as clearly a lower concentration of Ca^{2+} ($\approx$0.1 mM) is required compared to Ba^{2+} ($\approx$1 mM). The binding constant is related to the size of the cation, also taking into account its hydration shell. We can suppose that for both cation complexes, one molecule of the dimer is slightly shifted compared to the other, with the two crowns being slightly tilted. Consequently, the larger Ba^{2+} cation would be closer to the amino group of one ligand than the other, thus affecting one hemicyanine (Figure 13). We believe that, owing to strong π–π interactions, molecules organised in the monolayer at the air–water interface preserve such an arrangement when cations leave the crown ether upon chloroform evaporation.

3. Conclusions

The properties of the crown-substituted hemicyanine dye **C1** were investigated in solvents of different dielectric constants, and in solutions containing alkaline-earth-metal cations. The PCT behaviour of **C1** in solution was demonstrated. Upon excitation, **C1** undergoes a net displacement of electron density from the lone-pair-bearing amine moiety towards the electron-poor pyridinium moiety. The dipole-moment change between ground and excited states was calculated to be 11 D according to the Lippert–Mataga theory, and the result was confirmed by using quantum chemical calculations.

For both Ca^{2+} and Ba^{2+}, the binding constant for 2:1 complexation (K_{21}) in acetonitrile was determined to be approximately 10^7 M^{-1}, whereas the constant for 1:1 complexation (K_{11}) was too low to obtain a reliable data fit. The asymmetric sandwich-dimer model, in which two hemicyanine molecules share one cation was proposed, and the existence of such dimers in solution was supported by transient absorption and fluorescence anisotropy experiments.

The monolayers and LB films of an amphiphilic analogue (**C2**) of this aza-crown-substituted hemicyanine were also studied in relation to their interaction with cations leading to excimer formation. It was shown that the presence of Ca^{2+} and Ba^{2+} cations in the subphase inhibits the H-aggregation process in **C2** monolayers. Surface-pressure-controlled reversible excimer formation at the air–water interface in the presence of cations was demonstrated. Excimer-type emission of **C2** LB films transferred from the cation-containing subphase was also monitored by using fluorimetry and fluorescence microscopy, and a supramolecular structure responsible for this type of emission in monolayers and LB films was proposed. Sandwich-type dimers formed through cation binding upon spreading of the monolayer, appear to be retained after the evaporation of chloroform, despite the fact that hydration of the crown ether ejects cations from the monolayer. The subsequent compression of the monolayer induced specific orientation and provided a close-packing organisation of pre-formed dimers at the air–water interface. Evidently, such organisation favoured the formation of excimers.

It was shown that hemicyanine monolayers behave similarly in the presence of Ca^{2+} and Ba^{2+}. The major difference between the two cations is the concentration range necessary to induce a specific effect of excimer formation: approximately 0.1 and 1 mM for Ca^{2+} and Ba^{2+}, respectively.

Finally, photosensitive, cation-responsive films have been formed and studies showed encouraging results towards the development of artificial membranes.

Experimental Section

Dyes

The syntheses of hemicyanine dyes 1-methyl-4-{(*E*)-2-[4-(1,4,7,10-tetraoxa-13-azacyclopentadecane-13-yl)phenyl]vinyl}pyridinium perchlorate (**C1**) and 1-docosyl-4-{(*E*)-2-[4-(1,4,7,10-tetraoxa-13-azacyclopentadecane-13-yl)phenyl]vinyl}pyridinium perchlorate (**C2**; Figure 1) have been described previously.[30,32] The crown ether moiety confers its molecular recognition capacity to the dye, the size of the cavity being well suited for Ca^{2+}. The alkyl substituent ($C_{22}H_{45}$) in **C2** allows the molecule to form organised monolayers at the air water interface, owing to entropic contributions and van der Waals interactions. For reasons of solubility, effects of the solvents on the optical properties of the hemicyanines were studied by using the **C1** analogue, which bears a CH_3 group instead of a long alkyl chain.

Steady-State Electronic Absorption and Fluorescence in Solution

Stock solutions of the dyes (5 mM) were prepared in acetonitrile. They were diluted in solvents of the highest available purity (Merck, Darmstadt, and Nuka, Neu-Ulm): benzene, ethyl acetate, EGDME, MIBK, acetone, acetonitrile, DMSO, PC and Millipore water (pH 5.5, resistivity $>$ 18.2 MΩ cm ^{1}). The static dielectric constants of these solvents at 25 °C are listed in Table 1. Absorption and fluorescence emission spectra were recorded by using a 1 cm silica cell, on a Cary 5G UV/Vis/NIR spectrophotometer (Varian) and a Fluorolog spectrofluorimeter (Jobin Yvon, Longjumeau, France), respectively. The dipole moments were obtained from quantum chemical computations by using the PM6 Hamiltonian included in MOPAC software.[21]

Complexation studies were performed in order to determine the stoichiometry of the Ba^{2+} and Ca^{2+} hemicyanine complexes. The ratio of Ba^{2+} or Ca^{2+} to the dye was increased by adding aliquots (2 10 µL) of a solution of the corresponding perchlorate salt (10^{-3} M 10^{-1} M) to a solution of the hemicyanine (2.5×10^{-5} M in acetonitrile). The binding constants of the complexes were determined from the absorption spectra, by using the SPECFIT/32 program.[22]

Surface Pressure Measurements

Surface pressure measurements were carried out in air by using a 601M Nima Langmuir trough (approximately 19×12×0.5 cm) equipped with a Wilhelmy balance (Nima, Coventry, United Kingdom). Pure Millipore water or aqueous solutions of Ba^{2+} or Ca^{2+} perchlorates (0 10 mM) were used as the subphase. Hemicyanine **C2** (Figure 1) was dissolved in chloroform at a concentration between 0.5 1 mM and spread over the air water interface. After

the evaporation of chloroform (15 min), the monolayers were compressed continuously at a rate of 15 $cm^2 min^{-1}$. The temperature of the subphase was kept constant to $20 \pm 1\,^{\circ}C$. All of these experiments were performed under red light, in order to limit undesired photoreactions.

Fibre-Optic Absorption Spectroscopy

Absorption spectra of monolayers on an aqueous subphase were recorded over the wavelength range 240 750 nm by using an AvaSpec-2048 FT-SPU fibre-optic spectrophotometer (Avantes, Apeldoorn, Netherlands). A UV/Vis reflectometric probe with a fibre diameter of 400 μm, combined with a six-fibre irradiating cable was located perpendicularly to the subphase surface at a distance of 2 3 mm from the monolayer. The signal obtained upon light reflection from the subphase surface immediately before monolayer spreading, was used as a baseline measurement. This method allowed us to obtain UV/Vis spectra of monolayers with high enough intensity and resolution to distinguish even minor spectral changes. This technique is described in detail elsewhere.[33]

Fibre-Optic Fluorimetry

During the compression, fluorescence spectra of hemicyanine monolayers were obtained by using an AvaSpec-2048 fibre-optic spectrophotometer. A UV/Vis reflectometric probe with a fibre diameter of 600 μm was placed perpendicularly at 2 3 mm to the monolayer surface. Additional light-emitting diodes were used with an emission band as close as possible to the principal absorption band of the dye molecules in the monolayer. The light-emitting diodes were placed directly above the monolayer to ensure a 45° angle of incidence of the exciting light on the subphase surface.

LB Film Deposition and Characterisation

For LB transfers, a silica plate was immersed into the Langmuir trough, perpendicular to the interface, before spreading the hemicyanine chloroform solution. The monolayer was compressed to the desired surface pressure, which was kept constant by means of a control system permanently adapting the monolayer surface. In the case of hemicyanine monolayers, the surface pressure decreased slightly during the period of 10 15 min, which is attributed to a reorganisation of molecules at the air water interface. After this stabilisation period, the silica plate was removed from the water at a constant speed of 20 mm min^{-1}, which resulted in a hemicyanine monolayer being transferred on both sides of the plate. All of these experiments were performed under red light, in order to limit undesired photoreactions.

Absorption and fluorescence emission spectra of LB films were acquired with the Cary 5G UV/Vis/NIR spectrophotometer and the Fluorolog spectrofluorimeter, respectively.

Transient Absorption and Time-Resolved Fluorescence

The laser system [Ti:sapphire laser (Femtolasers, Vienna, Austria) optically pumped with Nd:YAG laser at 532 nm (Coherent, Santa Clara, USA)] generated pulses of 30 fs centred at 800 nm (800 μJ, 1 kHz repetition rate). The laser output was split into two, to produce the pump and the probe beams. 80% of pulses were used to pump an optical parametric generator [TOPAS (Light Conversion, Vilnius, Lithuania)] to generate the wavelength-tuneable pump pulse. Following TOPAS, the harmonic generation or frequency mixing in a nonlinear crystal produced excitation pulses in the range 250 2600 nm. The probe was a white-light continuum pulse, extending from 390 to 900 nm, and was generated by focusing the 800 nm pulses (~5 μJ per pulse) into a 5 mm-thick D_2O cell. Part of the probe pulse was split off for reference before interaction with the sample and was directed into the AvaSpec spectrometer coupled with a charge-coupled device (CCD) array by means of an optical fibre. The remaining part of the continuum was used as a probe pulse to monitor the transient absorption spectra of the sample at different time delays (Δt) between the pump pulse and the continuum probe pulse. The transient absorption spectrum was determined in the presence and in the absence of the pump pulse, controlled by a shutter, at a given time delay between the pump and the probe pulses with an error of about 0.005 for the optical density.

Fluorescence Anisotropy

Fluorescence anisotropy was measured using a linearly polarised excitation pulse. The fluorescence polarisation, before being sent to the spectrograph, was analysed using a thin-film polariser. The fluorescence anisotropy decay r was obtained using the Equation (1):

$$r \quad \frac{I_{\parallel} \quad I_{\perp}}{I_{\parallel} + 2I_{\perp}} \tag{1}$$

where $I_{||}$ is the decay of fluorescence with parallel polarisation with respect to the excitation and $I_{\perp}$ is the perpendicularly polarisation fluorescence decay. The high dynamic range of fluorescence intensity measurements made it possible to determine molecular reorientation times up to 350 ps for LDS750, TPP and stilbene 420. The uncertainty of these measurements was better than 3 ps for the fastest reorientation time.

The data was treated according to Langevin's equation that was applied assuming solvent friction in solution as an external force. In this model, the total torque acting on the molecule is separated into the frictional torque, which is proportional to the angular velocity of the molecule, and a random torque [Eq. (2)]:[34,35]

$$I\frac{\partial}{\partial x}\vec{\omega}(t) \quad \xi I\vec{\omega}(t) + \vec{T} \tag{2}$$

where $\vec{\omega}(t)$ is the angular velocity, ξ is the microscopic friction of solvent, I is the moment of inertia of solute and $\vec{T}$ is the torque. After using the stochastic solution of Langevin equation and the continuum hydrodynamic model, considering the timescale of the molecular motion, the equation for anisotropy decay can be simplified as follows [Eq. (3)]:

$$r(t) \quad C\exp\left(\frac{6kT\tau}{I\xi}\right) \tag{3}$$

and anisotropy decay time τ can be expressed as Equation (4):

$$\tau \quad \frac{I\xi}{6kT\tau} \tag{4}$$

Fluorescence Microscopy

LB films transferred onto silica substrates were placed on the stage of a fixed-stage upright microscope (Olympus BX51WI) equipped with a 100 W mercury lamp (U-LH100HG), a BX-RFA illuminator and

an U-MNB2 filter cube (excitation 470 490 nm, emission >520 nm). An LMPF1 ×10 objective was used. Images were recorded with a Color View II CCD camera from SIS (Olympus-Soft Imaging Solutions, Münster, Germany). Acquisition times were typically 1 5 s. Several images were systematically taken at different positions on the LB films. The lateral resolution of the setup was in the 0.4 0.6 μm range.

Acknowledgements

Financial support from the Ministère de la Recherche et de l'Enseignement Supérieur; Université de Bordeaux; the Russian Academy of Sciences Presidium P8(5) program and the program of cooperation between the Russian Academy of Sciences and the French Centre National de la Recherche Scientifique (CNRS) is gratefully acknowledged.

Keywords: excimers · hemicyanines · fluorescence spectroscopy · ion-sensitive membranes · Langmuir–Blodgett films

[1] S. Tatay, P. Gaviña, E. Coronado, E. Palomares, *Org. Lett.* **2006**, *8*, 3857 3860.
[2] Y. Shiraishi, R. Miyamoto, T. Hirai, *Langmuir* **2008**, *24*, 4273 4279.
[3] L. Rivera, M. Puyol, S. Miltsov, J. Alonso, *Anal. Bioanal. Chem.* **2007**, *387*, 2111 2119.
[4] J. Bricks, *J. Photochem. Photobiol. A* **2000**, *132*, 193 208.
[5] E. V. Tulyakova, O. Fedorova, Y. V. Fedorov, G. Jonusauskas, V. Anisimov, *J. Phys. Org. Chem.* **2008**, *21*, 372 380.
[6] J. F. Callan, A. P. de Silva, D. C. Magri, *Tetrahedron* **2005**, *61*, 8551 8588.
[7] F. Ito, T. Nagamura, *J. Photochem. Photobiol. C* **2007**, *8*, 174 190.
[8] S. A. Soper, Q. L. Mattingly, *J. Am. Chem. Soc.* **1994**, *116*, 3744 3752.
[9] S. Das, K. G. Thomas, K. J. Thomas, P. V. Kamat, M. V. George, *J. Phys. Chem.* **1994**, *98*, 9291 9296.
[10] J. M. Lanzafame, A. A. Muenter, D. V. Brumbaugh, *Chem. Phys.* **1996**, *210*, 79 89.
[11] C. F. Zhao, R. Gvishi, U. Narang, G. Ruland, N. P. Prasad, *J. Phys. Chem.* **1996**, *100*, 4526 4532.
[12] G. Marowsky, L. F. Chi, D. Möbius, R. Steinhoff, Y. R. Shen, D. Dorsch, B. Rieger, *Chem. Phys. Lett.* **1988**, *147*, 420 424.
[13] C. Grauby Heywang, S. Selector, E. Abraham, G. Jonusauskas, *Prot. Met. Phys. Chem. Surf.* **2011**, *47*, 31 38.
[14] A. Lambacher, P. Fromherz, *J. Phys. Chem. B* **2001**, *105*, 343 346.
[15] R. Rizzuto, T. Pozzan, *Physiol. Rev.* **2006**, *86*, 369 408.
[16] a) T. Gunnlaugsson, M. Glynn, G. M. Tocci, P. E. Kruger, F. M. Pfeffer, *Coord. Chem. Rev.* **2006**, *250*, 3094 3117; b) D. T. McQuade, A. E. Pullen, T. M. Swager, *Chem. Rev.* **2000**, *100*, 2537 2574; c) A. Ion, I. Ion, A. Popescu, M. Ungureanu, J. C. Moutet, E. Saint Aman, *Adv. Mater.* **1997**, *9*, 711 713; d) M. A. Kalinina, N. V. Golubev, O. A. Raitman, S. L. Selector, V. V. Arslanov, *Sens. Actuators B* **2006**, *114*, 19 27.
[17] P. Fromherz, *J. Phys. Chem.* **1995**, *99*, 7188 7192.
[18] E. V. Lippert, *Z. Elektrochem.* **1957**, *61*, 962 975.
[19] N. Mataga, S. Nishikawa, T. Asahi, T. Okada, *J. Phys. Chem.* **1990**, *94*, 1443 1447.
[20] P. Suppan, *J. Photochem. Photobiol. A* **1990**, *50*, 293 330.
[21] J. J. P. Stewart, MOPAC2009, Stewart Computational Chemistry, Colorado Springs, CO, USA, **2008**.
[22] UV/Vis titrations were analysed by fitting the whole series of spectra using the software SPECFIT. The SPECFIT program analyses equilibrium data sets using singular value decomposition and linear regression modelling by the Levenberg Marquardt method to determine a cumulative binding constant; H. Gampp, M. Maeder, C. J. Meyer, A. D. Zuberbühler, *Talanta* **1986**, *33*, 943.
[23] a) M. Mitewa, N. Mateeva, L. Antonov, T. Deligeorgievt, *Dyes Pigm.* **1995**, *27*, 219 225; b) N. Mateeva, V. Enchev, L. Antonov, T. Deligeorgiev, M. Mitewa, *J. Inclusion Phenom. Mol. Recognit. Chem.* **1994**/**1995**, *20*, 323 333; c) M. V. Alfimov, A. V. Churakov, Y. V. Fedorov, O. A. Fedorova, S. P. Gromov, R. E. Hester, J. A. K. Howard, L. G. Kuz′mina, I. K. Lednev, J. N. Moore, *J. Chem. Soc. Perkin Trans. 2* **1997**, 2249 2256; d) M. Hiraoka *Crown Compounds: Their Characteristics and Application*, Elsevier, New York, **1982**.
[24] R. Mathevet, G. Jonusauskas, C. Rulliere, J. F. Letard, R. Lapouyade, *J. Phys. Chem.* **1995**, *99*, 15709 15713.
[25] M. M. Martin, P. Plaza, Y. H. Meyer, F. Badaoui, J. Bourson, J. P. Lefèvre, B. Valeur, *J. Phys. Chem.* **1996**, *100*, 6879 6888.
[26] O. Kühn, V. Chernyak, S. Mukamel, *J. Chem. Phys.* **1996**, *105*, 8586 8601.
[27] S. J. Rosenthal, X. H. Xie, M. Du, G. R. Fleming, *Chem. Phys.* **1991**, *95*, 4715 4718.
[28] S. L. Selektor, O. A. Raitman, D. A. Silant′eva, N. V. Ivanova, G. Jonusauskas, E. V. Lukovskaya, P. Batat, V. V. Arslanov, *Prot. Met. Phys. Chem. Surf.* **2011**, *47*, 484 493.
[29] X. Lu, K. Han, S. Ma, G. Wang, W. Wang, *Proc. SPIE* **1996**, *2897*, 36 42.
[30] A. A. Abramov, *Vestn. Mosk. Univ. Ser. 2 Khimiya,* **2000**, *41*, 3 15.
[31] D. A. Silantyeva, S. L. Selector, J. N. Malakhova, A. V. Bakirov, M. A. Shcherbina, S. N. Chvalun, N. K. Ibrayev, G. Jonusauskas, V. V. Arslanov, IV International Conference on Colloid Chemistry and Physicochemical Mechanics, Book of abstracts, Moscow, Russia, **2013**, 41 43.
[32] J. P. Dix, F. Voegtle, *Chem. Ber.* **1980**, *113*, 457 470.
[33] S. D. Stuchebryukov, S. L. Selektor, D. A. Silantieva, A. V. Shokurov, *Prot. Met. Phys. Chem. Surf.* **2013**, *49*, 189 197.
[34] J. S. Baskin, *Chem. Phys. Lett.* **1997**, *275*, 437 444.
[35] J. S. Baskin, M. Chachisvilis, M. Gupta, A. H. Zewail, *J. Phys. Chem. A* **1998**, *102*, 4158 4171.